AIAA JOURNAL
Vol. 31, No. 1, January 1993

New Wall Treatment for Numerical Navier-Stokes Solution of Incompressible Turbulent Flows

Jean Caillé*
Algorithme Informatique, Inc., Ville Mont-Royal, Quebec H3P 3E5, Canada
and
Joseph A. Schetz†
Virginia Polytechnic Institute and State University, Blacksburg, Virginia 24061

A new treatment of the near-wall region is presented for the numerical computation of two-dimensional and three-dimensional incompressible turbulent flows. The idea is to enforce conservation of mass and momentum over a thin layer in the innermost region of the wall viscous layer expressed as an integral condition. The flow is solved down to the wall with a slip velocity using the Navier-Stokes equations and following the idea of a pseudolaminar analysis developed by Clauser, and the wall shear stress is imposed as a boundary condition on the surface. A two-layer model is not required to represent turbulent transport. The inner strip integral method uses values for the pressure gradient and the velocity and shear at the outer edge of the inner strip from the Navier-Stokes solution and updates the value for the wall shear stress for the Navier-Stokes solution until convergence is achieved. This procedure is more soundly based than and is not equivalent to the well-known wall function method. A computational procedure was developed for flows in or about two-dimensional and three-dimensional geometries. The Reynolds-averaged Navier-Stokes equations with the Clauser outer region eddy viscosity model are solved using the finite element method with a penalty formulation in this implementation of the new approach. The validation of the approach was done by comparing the present numerical predictions with the measurements of well-known experiments, including cases with strong adverse pressure gradients. Only 15–20 nodes normal to the wall are required for the Navier-Stokes solution to obtain accurate predictions.

Nomenclature

A	= normalized wall shear stress
C_1	= constant in modified law of the wall
C_f	= skin-friction coefficient
C_{mc}	= slope constant in crosswise velocity profile
d	= characteristic dimension
H	= upper limit of control volume
n_j	= normal components
p	= pressure
R_i	= residuals
Re_d	= Reynolds number based on d
u_i	= velocity components
t_i	= surface tractions
U, W	= orthogonal velocity components
U_e	= edge velocity
u, v, w	= Cartesian velocity components
u_*	= friction velocity
x, y, z	= Cartesian coordinates
β_w	= wall crossflow angle
δ	= boundary-layer thickness
δ^*	= displacement thickness
δ_1	= streamwise displacement thickness
η	= nondimensionalized normal coordinate
κ	= law of the wall constant
λ	= penalty parameter
μ	= laminar viscosity
μ_T	= eddy viscosity
ν	= kinematic viscosity
ρ	= density
τ	= shear stresses

Subscripts

H	= upper limit of inner strip
mc	= maximum crosswise velocity location
w	= wall

Presented as Paper 91-1736 at the AIAA 22nd Fluid Dynamics, Plasma Dynamics, and Lasers Conference, Honolulu, HI, June 24–26, 1991; received July 15, 1991; revision received April 18, 1992; accepted for publication April 18, 1992.

*President. Member AIAA.
†W. Martin Johnson Professor and Head, Aerospace and Ocean Engineering Department. Fellow AIAA.

Introduction

ACCURATE and numerically efficient treatment of the very-near-wall region in turbulent flows remains an important issue. The matter is greatly aggravated for three-dimensional flows, where storage and computational time problems present severe difficulties even for researchers with easy access to the largest machines. The issue is significant for three-dimensional boundary-layer methods and much more critical for three-dimensional Navier-Stokes formulations.

To this point, there have been three general approaches. The first is simply to enforce the no-slip boundary condition on the wall and employ a multilayer turbulent transport model. This quickly leads to the memory and time problems cited earlier, especially for three-dimensional cases. The second and third approaches that have been developed in the past attempt to alleviate these problems in an approximate way, and they are similar, but are not the same. One method[1] solves down to the wall and enforces the no-slip boundary condition, but with a coarse mesh. That precludes finding the wall shear using a numerically calculated velocity derivative at the wall. Rather, a velocity profile shape is presumed known in the form of a law of the wall, and the wall shear is found by matching the slope in a region away from the wall. The procedure is similar to Clauser's method for finding wall shear from a measured velocity profile. The other common method is the so-called wall function method.[2] The first point of the numer-

ical solution is at a location above the wall, and the solution is matched to a law of the wall velocity profile at that point. Both of these approximate methods work well for two-dimensional flows over smooth, solid surfaces at low speeds with no separation where the law of the wall is well known. As soon as any of these limitations is violated, these methods perform poorly, because there are no sound, generally accepted extensions to the law of the wall for such cases. This represents a severe restriction, since, in two-dimensional cases, for example, one can easily now use the full formulation, and no approximate method is needed at all.

Based on the preceding discussion, it was decided that a new, more general, physically sounder method for treating the wall zone in an approximate but accurate way was needed, especially for three-dimensional flows. There are two basic parts to the new treatment proposed here. The first key concept is the enforcement of conservation of mass and momentum in an integral sense in a thin, innermost zone within the total wall viscous layer. This is an extension of one part of the successful Moses integral method for two-dimensional boundary-layer flows.[3] The integral method has recently been extended to three-dimensional boundary-layer flows.[4] Here, we are using these ideas only in the innermost part of the wall zone and are not restricting the approach to boundary-layer flows. To enforce conservation of mass and momentum in this inner layer in an integral sense, it is necessary to have an assumed velocity profile shape. We have used the well-tested three-dimensional law of the wall suggested by Johnston. One might now incorrectly conclude that the proposed new approach collapses back to the older wall function method. That is not the case. It is well known that enforcing integral conditions dramatically reduces the sensitivity of the results to the specific profile shape assumed. In the wall function method one needs to know the value of the velocity itself at a fixed point above the wall; doing so requires great precision in the assumed profile. In the new method we need only the value of integrals of the velocity profile from the wall up to a point above the wall; this requires much less precision in the assumed profile. Also, enforcing conservation of mass and momentum over the whole innermost part of the wall layer will ensure more realistic results over the wall function method, which enforces no such global constraint. The numerical solution for the outer region of the wall viscous layer is coupled to the inner region solution through the wall shear, which is imposed as a boundary condition at the wall on the outer region solution.

The second important part of the new approach concerns turbulence modeling. The numerical solution for the outer region is carried down to the wall with an imposed boundary condition on the shear; this implies velocity slip at the wall and is reminiscent of Clauser's analysis of the outer region of a boundary layer, where he developed his outer region eddy viscosity model treating the outer region flow as pseudolaminar with slip velocity at the wall.[5] Clauser used the outer region eddy viscosity model all the way to the wall and found the wall shear using that value of the viscosity times the derivative of the pseudolaminar velocity profiles (with slip) at the wall. That procedure is also adopted here, which means that only an outer region turbulent transport model is needed.

A complete computational procedure was developed incorporating these ideas. The Reynolds-averaged, Navier-Stokes (RANS) equations are solved using the finite element method (FEM) with a penalty formulation. The method could as easily have been used with a finite difference or finite volume method. The turbulence transport is currently modeled with a Clauser outer region eddy viscosity model extended to three dimensions. Other models, such as mixing length, turbulent kinetic energy (TKE), and k-ϵ, can be accommodated. The basic approach developed here is independent of the numerical method or the turbulence model to be used. About 15–20 nodes across the whole wall viscous layer are sufficient. The wall shear stress is imposed as a boundary condition at the wall. First, the Navier-Stokes solver is run with an estimated value of the wall shear. Second, the pressure gradient and the velocity and shear at the edge of the thin layer are taken from the RANS solution and used for the inner layer integral solution. This yields updated values for the wall shear, which are used for the next RANS solution. The whole process converges very quickly.

The validation of the method was done by comparing the present numerical results with the measurements of well-known two-dimensional and three-dimensional experiments. Three flows were studied for the two-dimensional analysis: 1) the flow over a flat plate (Wieghardt-Tillmann), 2) the flow over a flat surface with a moderate adverse pressure gradient (Samuel-Joubert), and 3) the flow about an airfoil-like body with a strong adverse pressure gradient (Schubauer-Klebanoff). For the three-dimensional analysis, two flows were chosen: 1) the flow over a flat surface with a 35-deg sweep angle under infinite swept-wing conditions in an adverse pressure gradient (Van den Berg-Elsenaar) and 2) the flow over a flat surface with an adverse pressure gradient in the streamwise direction and an induced pressure gradient in the crosswise direction (Müller-Krause).

Navier-Stokes Solver

Equations

The mathematical model consists of the continuity equation and the RANS equations with the Reynolds stresses defined by the Boussinesq assumption:

$$u_{i,i} = 0 \tag{1a}$$

$$\rho u_j u_{i,j} = -p_{,i} + [(\mu + \mu_T)(u_{i,j} + u_{j,i})]_{,j} \tag{1b}$$

Turbulence Model

The eddy viscosity model is only required for the outer region of the viscosity layer. The Clauser outer region model[5] was chosen because it has proven adequate in many previous works and because the extension to three-dimensional analysis is straightforward. For two-dimensional problems it is defined as

$$\mu_T = 0.0168 \rho U_e \delta^* \tag{2a}$$

For three-dimensional flows the model was chosen here as

$$\mu_T = 0.0168 \rho U_e \delta_1 \tag{2b}$$

where δ_1 is the streamwise displacement thickness that can be evaluated directly by integration of the velocity field.

Finite Element Formulation

The present work uses a weak Galerkin formulation for the FEM, with the pressure determined by a penalty approach. The complete details of this formulation are readily available; thus, only an outline of the technique is presented here.

Substitution of an approximation solution (u^*, p^*) into the equations yields a set of residual equations of the following form.

Momentum:

$$f_1(u^*, p^*) = R_1 \tag{3a}$$

Continuity:

$$f_2(u^*) = R_2 \tag{3b}$$

where R_i are the residuals, a measure of the quality of the approximate solution. The Galerkin method reduces this error to zero in a weighted sense by making the residuals orthogonal to some set of functions. The weighting functions ρu_i must satisfy the continuity equation. The continuity equation con-

straint is enforced by use of a penalty method. The resulting weak formulation is given by

$$\int_D \{\rho u_i \rho u_j u_{i,i} + \rho u_{i,i}(\mu + \mu_T)(u_{i,j} + u_{j,i}) + \lambda u_{i,i} \rho u_{i,i}\}\, dD = \int_S \{\rho u_i t_i\}\, dS \tag{4}$$

where λ is a positive number whose value affects the accuracy of the solution. A value of 10^6–10^8 usually proves effective. When the divergence theorem is applied, the natural boundary conditions involving the surface tractions are introduced:

$$t_i = [-p + (\mu + \mu_T)(u_{i,j} + u_{j,i})]n_j \tag{5}$$

The pressure appears only implicitly through the surface integrals on the right-hand side of Eq. (4). The only unknowns are the velocity components. Once the velocity field is obtained, the pressure may be computed in a postprocessing step from the following relationship:

$$p = -\lambda u_{i,i} \tag{6}$$

The formulation results in a system of nonlinear algebraic equations of the following form:

$$[K(u)]\{U\} = \{F\} \tag{7}$$

where K is the global system matrix, U is the global vector of unknown velocities, and F is the global vector of known boundary conditions. The successive substitution method was found suitable to solve this system of equations. The linearized system of equations is solved by direct Gaussian decomposition in a compacted, skyline, out-of-core solver.

For two-dimensional flows the biquadratic velocity, bilinear pressure quadrilateral element was used, and for three-dimensional flows the trilinear velocity, constant-pressure brick element was chosen for reasons of computational economy.

Boundary Conditions

One of the advantages of the FEM is the implementation of the boundary conditions. One can specify values for the velocity components or values for the surface tractions. For two-dimensional flows the velocity profile was known at the inlet; therefore, the values for the two velocity components were used as boundary conditions. For three-dimensional calculations the velocity was known for the inlet, the sides, and the top plane; therefore, the values for the three velocity components were used as boundary conditions. On all solid surfaces the wall shear stress components were input along with the zero normal velocity condition. Traction-free boundary conditions were used at the outlet of the domain and for an external flow outer boundary.

Two-Dimensional Strip-Integral Formulation

Momentum Integral Equation

Conservation of mass and conservation of momentum along the x axis are imposed on the control volume of finite height H and infinitesimal length, neglecting the pressure variation normal to the wall over the thin inner layer. The integral equation is then

$$\frac{d}{dx}\int_0^H u^2\, dy - u_H \frac{d}{dx}\int_0^H u\, dy = \frac{-H}{\rho}\frac{dp}{dx} + \frac{\tau_H - \tau_w}{\rho} \tag{8}$$

where u_H and τ_H are the velocity and the shear stress at the upper limit of the strip, respectively, and τ_w is the wall shear stress. The pressure gradient was assumed constant over the inner strip but not over the whole viscous wall layer; it is evaluated from the Navier-Stokes solution at midstrip. It is different from the pressure gradient obtained from an inviscid solution, and the present method is not restricted to boundary-layer flows.

Velocity Profile

The applicability of an integral formulation depends on the parameterized velocity profile or, more specifically, on the shape of the profile. Good predictions do not require a perfect representation of the velocity, because the profile is integrated, and part of the error tends to be canceled out. The integral formulation is obtained for a strip going from the wall to a location inside the so-called overlap region. Thus, the law of the wall adequately represents the velocity profile over the entire strip. The law of the wall is usually written as

$$\frac{u}{u^*} = \frac{1}{\kappa}\ell n\left(\frac{yu_*}{\nu}\right) + C \tag{9}$$

with $\kappa = 0.41$ and $C = 4.9$ (Ref. 5). Using d and rearranging the previous equation, one gets

$$\frac{u}{U_e} = A\, \ell n(C_1 A Re_d \eta) \tag{10}$$

with

$$C_1 = 3.06, \quad A = u_*/\kappa U_e, \quad Re_d = U_e d/\nu, \quad \eta = y/d$$

The parameter A can be interpreted as a normalized wall shear stress. The usual choice for d is δ. However, in the present work the characteristic dimension is obtained from the Navier-Stokes solution, and it is more accurate to extract the displacement thickness than the boundary-layer thickness from the velocity field. Therefore, the velocity profile used in the integral equation is

$$\frac{u}{U_e} = A\, \ell n(C_1 A Re_{\delta^*}\eta) \quad \text{with} \quad \eta = y/\delta^* \tag{11}$$

Differential Equations

After integration of the velocity profile and expansion of the derivatives, the following form is obtained for the ordinary differential equation from Eq. (8):

$$\frac{dA}{dx} = f\left(x,\ U_e,\ A,\ Re_{\delta^*},\ \eta_H,\ u_H,\ \tau_H,\ \frac{dp}{dx}\right) \tag{12}$$

All of the information is readily available from the Navier-Stokes solution except the unknown A. The choice of η_H is arbitrary. A value in the range [1.0, 3.0] proved effective.

Starting from the initial location where the value of the skin-friction coefficient is known, the solution is computed for the normalized wall shear stress along the wall using a second-order Runge-Kutta space-marching technique.

Three-Dimensional Strip-Integral Formulation

Momentum Integral Equations

Conservation of mass and conservation of momentum in the x and z directions are imposed on the control volume of finite height H and infinitesimal base dx, dz, neglecting the pressure variation normal to the wall. The set of two integral equations that result written in Cartesian coordinates is then

$$\frac{\partial}{\partial x}\int_0^H u^2\, dy + \frac{\partial}{\partial z}\int_0^H uw\, dy - u_H\left[\frac{\partial}{\partial x}\int_0^H u\, dy + \frac{\partial}{\partial z}\int_0^H w\, dy\right] = \frac{-H}{\rho}\frac{\partial p}{\partial x} + \frac{(\tau_{xH} - \tau_{xw})}{\rho} \tag{13a}$$

$$\frac{\partial}{\partial z}\int_0^H w^2\, dy + \frac{\partial}{\partial x}\int_0^H uw\, dy - w_H\left[\frac{\partial}{\partial x}\int_0^H u\, dy + \frac{\partial}{\partial z}\int_0^H w\, dy\right] = \frac{-H}{\rho}\frac{\partial p}{\partial z} + \frac{(\tau_{zH} - \tau_{zw})}{\rho} \tag{13b}$$

In previous studies it has been shown that streamline, non-orthogonal coordinates are better suited for the numerical integration of the three-dimensional momentum integral equations.

Velocity Profiles

The choice of the parameterized velocity profiles was based on the study of Ölcmen and Simpson.[6] Their review showed that Johnston's model was the best overall. A modified two-dimensional law of the wall is used for the streamwise velocity, whereas a "triangular model" relates the crosswise and streamwise velocities.[7] This model adequately represents the velocity profile over the entire strip. The velocity profiles are, respectively,

$$\frac{U}{U_e} = A \cos \beta_w \, \ell n(C_1 A Re_{\delta 1} \eta) \tag{14}$$

and

$$\frac{W}{U_e} = \frac{U}{U_e} \tan \beta_w \qquad \text{if} \qquad \eta < \eta_{mc} \tag{15a}$$

or

$$\frac{W}{U_e} = C_{mc}\left(1 - \frac{U}{U_e}\right) \qquad \text{if} \qquad \eta_{mc} < \eta \tag{15b}$$

with

$$C_{mc} = \frac{W_{mc}/U_e}{(1 - U_{mc}/U_e)}$$

where η_{mc} is the location of the maximum crosswise velocity.

Differential Equations

After integration of the velocity profiles and expansion of the derivatives for the two equations, the following form is obtained for the partial differential equations from Eqs. (13a) and (13b):

$$C_{11}\frac{\partial A}{\partial x} + C_{12}\frac{\partial \beta_w}{\partial x} = F_1 \tag{16a}$$

$$C_{21}\frac{\partial A}{\partial x} + C_{22}\frac{\partial \beta_w}{\partial x} = F_2 \tag{16b}$$

where the coefficients and the right-hand sides are functions of the unknowns (A and β_w) and quantities readily available from the Navier-Stokes solution. The right-hand sides also contain all of the derivatives with respect to the crosswise direction.

This set of equations is hyperbolic, and the characteristics are located between the external streamlines and the wall streamlines. The discretization of the surface must obey the Courant-Friedrichs-Lewy (CFL) condition, which requires that the computational domain of dependence include the physical domain of dependence. The numerical integration is done using a second-order Runge-Kutta scheme. Starting from the initial location, where the solution is known along the entire line, the solution is computed for the normalized wall shear stress and the wall crossflow angle over the wall using a space-marching technique. Boundary conditions are necessary at all locations where the flow enters the computational domain.

Computational Procedure

A flowchart of the computational procedure for the method is presented in Fig. 1. First, an inviscid solution is computed when required. It depends on the information available about the geometry and the flow conditions for the problem considered and the method available to obtain the initial guess for the wall shear stress and the eddy viscosity. An integral boundary-layer method can provide very good first approximations, reducing the number of iterations to reach the numerically "exact" solution. If an integral method is used, an inviscid solution is needed to provide an approximate edge velocity distribution. The inviscid flowfield is also a better initial velocity field to start the computation of the FEM Navier-Stokes solution compared to the common choice of a zero initial velocity field.

The Navier-Stokes solution is then computed using the approximate distribution for the wall shear stress and the eddy viscosity. The general purpose FEM program, FIDAP, (Ref. 8), is used as the Navier-Stokes solver here. The values for the

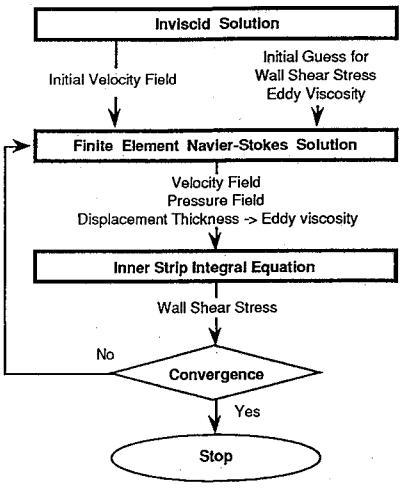

Fig. 1 Computational procedure for the method.

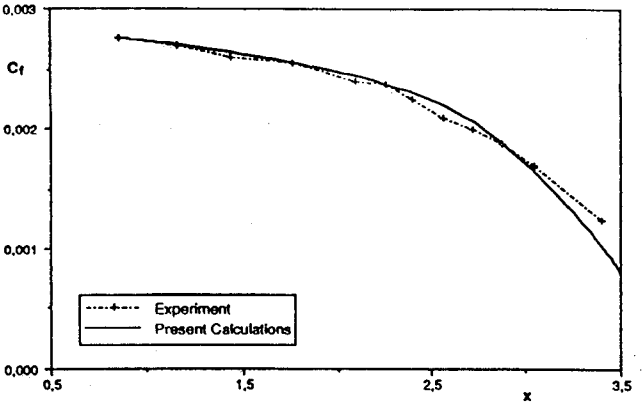

Fig. 2 Samuel-Joubert: skin-friction coefficient along the flat surface.

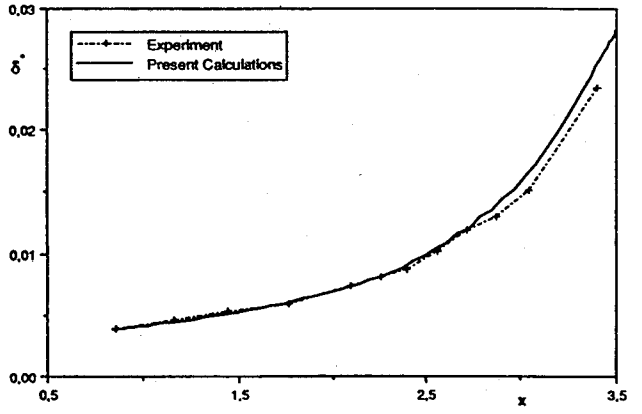

Fig. 3 Samuel-Joubert: displacement thickness along the flat surface.

velocity and the shear stress at the upper limit of the inner strip are extracted from the computed velocity field. The pressure gradient at midstrip is also extracted from the pressure field. With this information a corrected wall shear stress distribution is computed with the inner strip-integral method. This procedure is repeated until convergence. All computer programs were run on an IBM 3090 with vector facilities and extended architecture.

Two-Dimensional Results

A study of three different two-dimensional flows was made to check the validity and the practicality of the new computational procedure. These three flows were chosen because the experiments are well known since being chosen for the validation of different numerical methods at either the 1968 or the 1980–81 Stanford Conference.[9,10]

Wieghardt-Tillmann Flow

The first case is the flow over a thin flat plate with the experimental measurements taken by Wieghardt and Tillmann.[11] Good agreement was observed for both the skin friction and the displacement thickness.

Samuel-Joubert Flow

The second experiment is the flow over a flat surface with a moderate adverse pressure gradient performed by Samuel and Joubert.[12] The results for the skin-friction coefficient are shown in Fig. 2, and the results for the displacement thickness are shown in Fig. 3. The reader can note the level of agreement obtained. A deviation is seen near the end of the domain, when the pressure gradient becomes stronger, and the flow approaches separation.

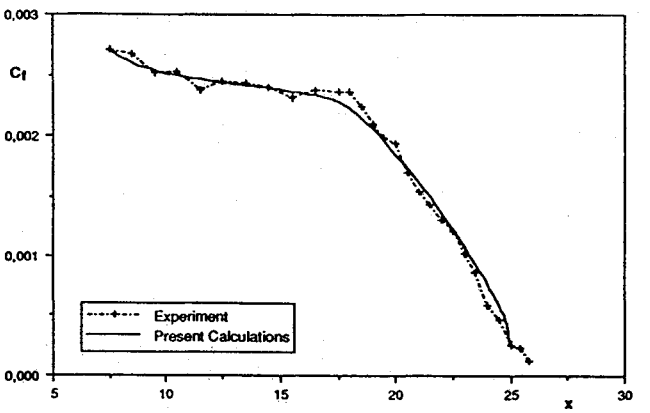

Fig. 4 Schubauer-Klebanoff: skin-friction coefficient along the body surface.

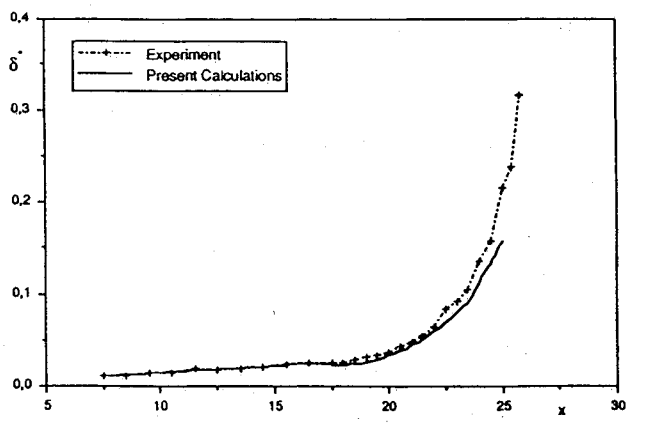

Fig. 5 Schubauer-Klebanoff: displacement thickness along the body surface.

Schubauer-Klebanoff Flow

The last case is the flow about an airfoil-like body with a strong adverse pressure gradient studied by Schubauer and Klebanoff.[13] The results for the skin-friction coefficient and the displacement thickness are shown in Figs. 4 and 5. The degree of agreement achieved with a relatively coarse mesh over the entire domain even when separation is approached can be seen.

Three-Dimensional Results

For the three-dimensional analysis two well-known and fully documented flows were chosen to validate the computational procedure. A study of three-dimensional turbulent boundary layers was done for the 1980–81 Stanford Conference,[10] which was followed in 1982 by a EUROVISC workshop.[14] The same two experimental investigations were chosen as test cases here for the validation of the new approach.

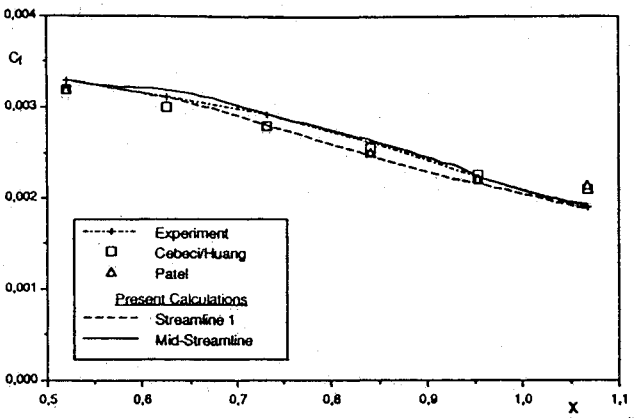

Fig. 6 Van den Berg-Elsenaar: skin-friction coefficient along the first and middle streamlines.

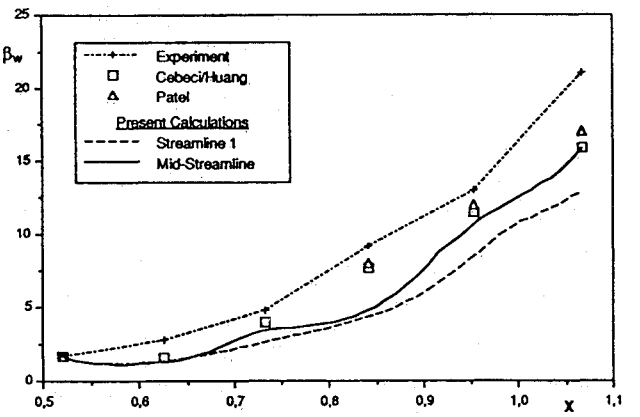

Fig. 7 Van den Berg-Elsenaar: wall crossflow angle along the first and middle streamlines.

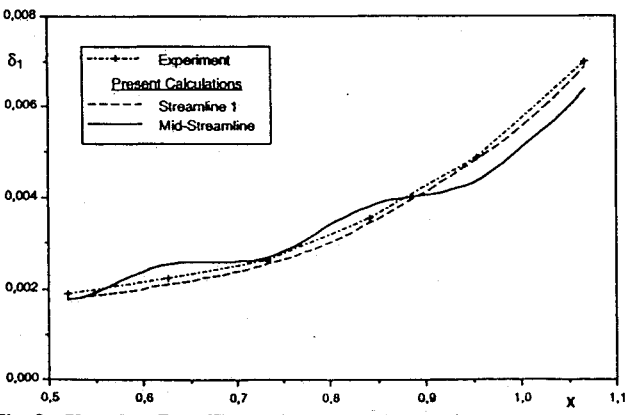

Fig. 8 Van den Berg-Elsenaar: streamwise displacement thickness along the first and middle streamlines.

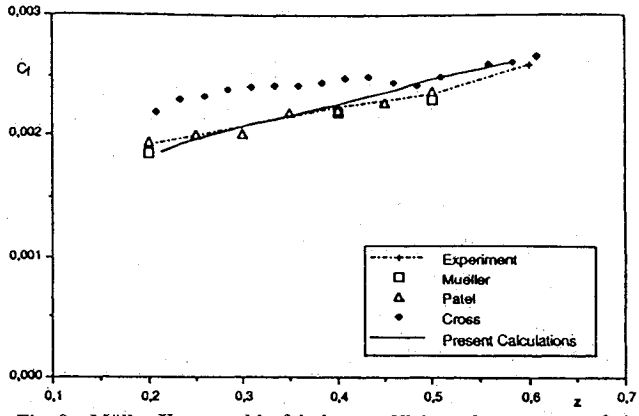

Fig. 9 Müller-Krause: skin-friction coefficient along z at $x = 0.4$.

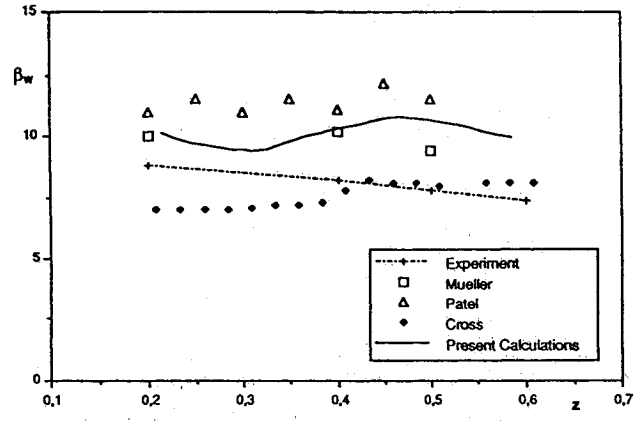

Fig. 10 Müller-Krause: wall crossflow angle along z at $x = 0.4$.

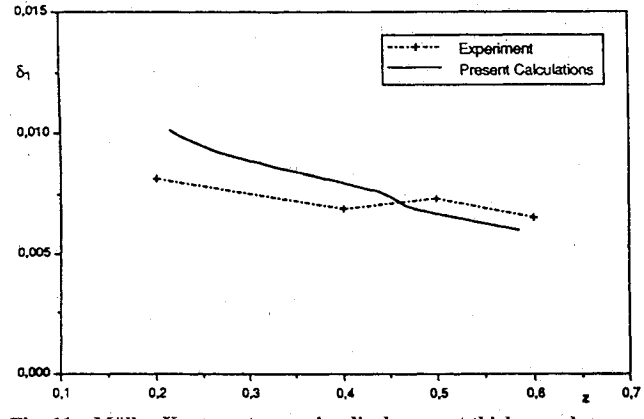

Fig. 11 Müller-Krause: streamwise displacement thickness along z at $x = 0.4$.

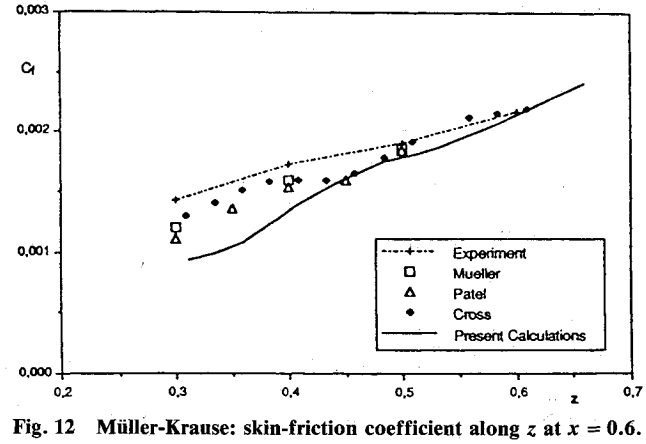

Fig. 12 Müller-Krause: skin-friction coefficient along z at $x = 0.6$.

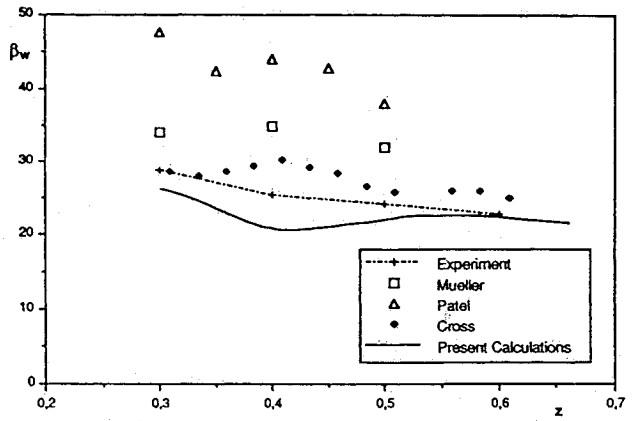

Fig. 13 Müller-Krause: wall crossflow angle along z at $x = 0.6$.

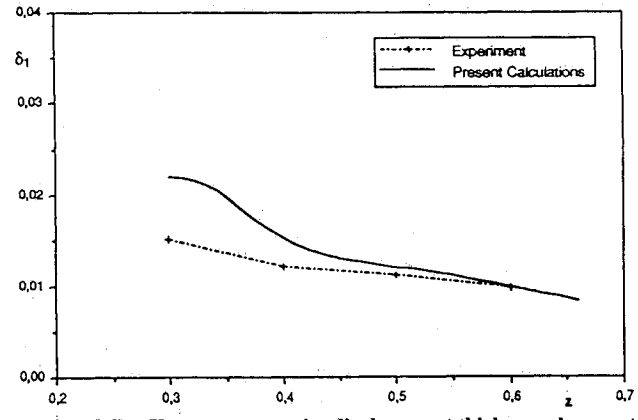

Fig. 14 Müller-Krause: streamwise displacement thickness along z at $x = 0.6$.

Van den Berg-Elsenaar Flow

Van den Berg and Elsenaar[15,16] investigated the flow over a flat surface with a 35-deg sweep angle under infinite swept-wing conditions in an adverse pressure gradient. The flow was computed for the first six stations. The results for the skin-friction coefficient, the wall crossflow angle, and the streamwise displacement thickness along two streamlines are shown in Figs. 6, 7, and 8, respectively, along with the results of two other differential methods.[14]

Müller-Krause Flow

The second case is the flow over a flat surface with an adverse pressure gradient in the streamwise direction and an induced pressure gradient in the crosswise direction studied by Müller and Krause.[17] The skin-friction coefficient, wall crossflow angle, and displacement thickness are shown in Figs. 9, 10, and 11, respectively, for the line $x = 0.4$, and in Figs. 12, 13, and 14, respectively, for the line $x = 0.6$, along with the results of three other methods.[14]

Conclusions

A new treatment of the near-wall region was developed for the computation of incompressible turbulent flows. By enforcing conservation of mass and momentum in the inner region in an integral sense, the physics of the flow is better represented than using the law of the wall in a wall function method. The flowfield is solved down to the wall with a slip velocity using the wall shear stress as the boundary condition. The value of the wall shear stress is corrected using a strip-integral method applied over a thin inner strip. There is no need for a two-layer turbulence model. Accurate predictions are obtained using only 15–20 nodes normal to the wall in the viscous layer. This is particularly important for three-dimensional computations.

A computational procedure was implemented using the FEM to solve the RANS equations for two-dimensional and

three-dimensional problems. The comparison of the present numerical results with two-dimensional experimental measurements showed comparable agreement for the skin-friction coefficient and the displacement thickness with the best competing differential methods achieved here on much coarser grids. We judge the three-dimensional results with the present method to be at least as good as any other method, and some of the other methods are integral methods utilizing considerable empirical input. The results with the present method are achieved using an approximate, but rational, wall zone treatment that permits using a coarse grid that results in substantial savings in storage requirements and computational time.

This new idea for the treatment of the wall region is simple and efficient. It can be practically implemented in a computational procedure with a finite difference, finite volume, or finite element method and applied to flows in or about two-dimensional and three-dimensional geometries. Any level of turbulent transport model can be incorporated. Predictions for three-dimensional problems can be obtained in a reasonable time considering the much smaller number of nodes required to describe the flow in the viscous layer. Finally, this general approach can be readily extended to compressible flow cases.

Acknowledgments

This work was supported mainly by the Office of Naval Research, with James Fein as Technical Monitor, and by the Cornell Theory Center, including the Cornell National Supercomputer Facility.

References

[1]Schetz, J. A., and Favin, S., "Numerical Calculation of Turbulent Boundary Layer with Suction or Injection and Binary Diffusion," *Astronautica Acta,* Vol. 16, Dec. 1971, pp. 339–351.

[2]Patankar, S. V., and Spalding, D. B., "A Calculation Procedure for Heat Transfer by Forced Convection Through Two-Dimensional Uniform-Property Turbulent Boundary Layers on Smooth Impermeable Walls," *Proceedings of the 3rd International Heat Transfer Conference,* Vol. II, American Institute of Chemical Engineers, Chicago, 1966, pp. 50–63.

[3]Moses, H. L., "A Strip-Integral Method for Predicting the Behavior of Turbulent Boundary Layers," *Proceedings of the 1968 Stanford Conference,* Vol. 1, 1969, pp. 76–82.

[4]Caillé, J., and Schetz, J. A., "Three-Dimensional Strip-Integral Method for Incompressible Turbulent Boundary Layers," AIAA Paper 90-1579, June 1990.

[5]Clauser, F. H., "The Turbulent Boundary Layer," *Advances in Applied Mechanics,* Vol. IV, Academic, New York, 1956, p. 51.

[6]Ölcmen, S., and Simpson, R. L., "Some Near Wall Features of Three-Dimensional Turbulent Boundary Layers," *Fourth Symposium on Numerical and Physical Aspects of Aerodynamic Flows,* 1989.

[7]Johnston, J. P., "On the Three-Dimensional Turbulent Boundary Layer Generated by Secondary Flow," *Journal of Basic Engineering,* Vol. 82, March 1960, pp. 233–248.

[8]Engelman, M. S., "FIDAP: A Fluid Dynamics Analysis Program," *Advances in Engineering Software,* Vol. 4, No. 4, Oct. 1982, p. 163.

[9]Coles, D. E., and Hirst, E. A., (eds.), *Proceedings Computation of Turbulent Boundary Layers 1968 AFOSR-IFS-Stanford Conference,* Vols. 1 and 2, Stanford Univ., Stanford, CA, 1969.

[10]Kline, S. J., Cantwell, B. J., and Lilley, G. M., (eds.), *1980–81 AFOSR-HTTM-Stanford Conference on Complex Turbulent Flows,* Vols. 1–3, Stanford Univ., Stanford, CA, 1981.

[11]Wieghardt, K., and Tillmann, W., "On the Turbulent Friction Layer for Rising Pressure," NACA TM 1314, 1951 (translation).

[12]Samuel, A. E., and Joubert, P. N., "A Boundary Layer Developing in an Increasingly Adverse Pressure Gradient," *Journal of Fluid Mechanics,* Vol. 66, Pt. 3, Nov. 1974, pp. 481–505.

[13]Schubauer, G. B., and Klebanoff, P. S., "Investigation of Separation of the Turbulent Boundary Layer," NACA TN 2133, 1950.

[14]Van den Berg, B., Humphreys, D. A., Krause, E., and Lindhout, J. P. F., "Three-Dimensional Turbulent Boundary Layers—Calculations and Experiments," *Notes on Numerical Fluid Mechanics,* Vol. 19, 1988.

[15]Van den Berg, B., and Elsenaar, A., "Measurements in a Three-Dimensional Incompressible Turbulent Boundary Layer in an Adverse Pressure Gradient Under Infinite Swept Wing Conditions," National Aerospace Lab., NLR TR 72092 U, The Netherlands, 1972.

[16]Van den Berg, B., Elsenaar, A., Lindhout, J., and Wesseling, P., "Measurements in an Incompressible Three-Dimensional Turbulent Boundary Layer, Under Infinite Swept-Wing Conditions, and Comparison with Theory," *Journal of Fluid Mechanics,* Vol. 70, Pt. 1, July 1975, pp. 127–148.

[17]Müller, U. R., "Measurements of the Reynolds Stresses and the Mean-flow Field in a Three-Dimensional Pressure-Driven Boundary Layer," *Journal of Fluid Mechanics,* Vol. 119, June 1982, pp. 121–153.